Title

Stabilization of reactive rare earth alkyl complexes through mechanistic studies.

Authors

Tanuhadi, Elias
Bair, Anna
Johnson, Mary
et al.

Publication Date

2024-11-25

DOI

10.1039/d4sc05983b

Peer reviewed

Chemical Science

ROYAL SOCIETY OF CHEMISTRY

EDGE ARTICLE

Cite this: DOI: 10.1039/d4sc05983b

All publication charges for this article have been paid for by the Royal Society of Chemistry

Stabilization of reactive rare earth alkyl complexes through mechanistic studies†

Elias Tanuhadi,[ab] Anna S. Bair,[ab] Mary Johnson,[ab] Philip Fontaine,[c] Jerzy Klosin,[*c] Sudipta Pal[c] and Polly L. Arnold[*ab]

Rare earth tris(alkyl) complexes such as $M(CH_2SiMe_3)_3(sol)_n$ are widely used as precursors for many compounds and as homogeneous catalysts for alkene polymerization and alkane functionalization. However, the thermal instability of those most conveniently made from the commercially available lithium salt of the neosilyl anion, $LiCH_2SiMe_3$, Li(r), restricts their utility. We present a new range of synthetically useful, more kinetically stable rare earth neosilyl solvates, derived from a full kinetic study of the various possible decomposition mechanisms of 7 known and 12 new solvated rare earth neosilyl complexes $M(CH_2SiMe_3)_3(sol)_n$, M = Sc(III), Y(III), Lu(III), Sm(III), and sol = THF; TMEDA; DMPE; diglyme ($(CH_3)_2(OCH_2CH_2)_2O$, **G2**), triglyme ($(CH_3)_2(OCH_2CH_2)_3O$, **G3**). Surprisingly, simply using higher-denticity donors to sterically disfavor neosilyl γ-H elimination is not effective. While $Sc(r)_3((CH_3)_2(OCH_2CH_2)_2O)$ has a half-life, $t_{1/2}$, of 258.1 h, six times longer than for $Sc(r)_3(C_4H_8O)_2$ ($t_{1/2}$ = 43 h), $Lu(r)_3((CH_3)_2(OCH_2CH_2)_2O)$ and $Y(r)_3((CH_3)_2(OCH_2CH_2)_2O)$ do not show the expected, analogous increased $t_{1/2}$. This is because new decomposition pathways appear for poorly fitting donors. Finally, kinetic studies demonstrate the impact of small, and increasing amounts of LiCl on the kinetics of the reactivity of the smaller alkyls $Y(r)_3(THF)_2$ and $Lu(r)_3(THF)_2$; molecules used in hydrocarbon chemistry and catalysis for fifty years. A new route to pure $Y(r)_3(THF)_2$, which avoids the traditional use of Li(r), is presented.

Received 4th September 2024
Accepted 30th October 2024

DOI: 10.1039/d4sc05983b

rsc.li/chemical-science

Introduction

Since their discovery in 1973,[1] neutral rare-earth metal complexes of the type $RE(CH_2SiMe_3)_3(THF)_x$, (RE = Sc, Y, Sm–Lu; x = 2, 3) featuring trimethylsilylmethyl ligands[2,3] have been valuable reagents for (pre)catalyst design, in particular for olefin- and diene polymerization,[4–7] and hydrocarbon C–H bond functionalization catalysis.[8,9] More recently, $RE(CH_2SiMe_3)_3(donor)_x$ (RE = Y, Dy, Er, Ho; donor = THF, quinuclidine, lutidine and $OPCy_3$) have shown promise as single molecule magnets.[10] Given that the Li and Mg salts of the trimethylsilylmethyl anion are commercially available, it is frustrating that all neosilyl complexes exhibit varying degrees of thermal instability, both in solution and in the solid state.[2] The larger –$CH(SiMe_3)_2$ alkyl[11] generates complexes with improved thermal stability, but its salts are not commercially available.

The employment of donor-ligands to enhance kinetic stability, but yet can be easily substituted by protic reagents,[12] should pave the way for novel RE-alkyl reactivity in these simple compounds.

Scheme 1 illustrates the three potential mechanisms for the elimination of $SiMe_4$ from $RE(CH_2SiMe_3)_3(THF)_2$. The first mechanism, Scheme 1a, involves the attack by a coordinated neosilyl on an α-CH_2 group. This results in the formation of a RE-alkylidene. However, this product has not been observed and is expected to be unstable. An early study of $Er(CH_2SiMe_3)_3(THF)_3$ suggested this decomposition mechanism, *via* silylalkylidene $[Er(CH_2SiMe_3)(CHSiMe_3)]_n$, but no evidence was provided to substantiate this, although this reactivity is well-documented for Ti.[13,14] The second mechanism, denoted as β-H in Scheme 1b, involves the attack by a neosilyl on a β-CH_2 group of a coordinated THF molecule, forming a metal vinyl alkoxide and ethylene, also anticipated to have low kinetic stability.[15,16] The third mechanism, Scheme 1c, involves the attack of the CH_2 carbon on a $SiCH_3$, forming a metallacycle. Deuterolysis experiments with $Lu(CH_2SiMe_3)_3(THF)_2$ suggested a γ-H elimination pathway to a metalacyclic intermediate $Me_2Si(\mu\text{-}CH_2)_2LuCH_2SiMe_3$ although this was not observed directly.[15]

The addition of diglyme, $(CH_3)_2(OCH_2CH_2)_2O$, **G2**, and glyme $(CH_3OCH_2)_2$, **G1**, to $Lu(CH_2SiMe_3)_3(THF)_2$ generated the unanticipated mixed solvates $Lu(CH_2SiMe_3)_3(\kappa^2\text{-}G_2)(THF)$ and

[a]Dept of Chemistry, University of California, Berkeley, Berkeley, CA, 94720, USA. E-mail: pla@berkeley.edu

[b]Chemical Sciences Division, Lawrence Berkeley National Laboratory, Berkeley, CA 94720, USA

[c]Corporate R&D, The Dow Chemical Company, Midland, Michigan 48674, USA. E-mail: jklosin@dow.com

† Electronic supplementary information (ESI) available: Synthetic and mechanistic details. CCDC 2351142–2351150, and 2369795. For ESI and crystallographic data in CIF or other electronic format see DOI: https://doi.org/10.1039/d4sc05983b

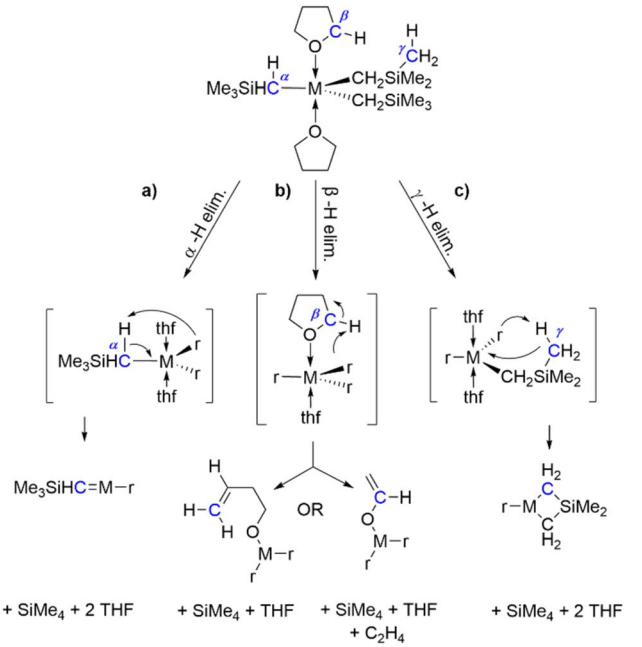

Scheme 1 The three possible mechanisms for elimination of $SiMe_4$ from $RE(r)_3(THF)_2$ (r = CH_2SiMe_3): (a) α-H elimination; (b) β-H elimination, and (c) γ-H elimination.

Table 1 Half-lives $t_{1/2}$ [h] of selected rare earth tris(neosilyl) solvates $RE(CH_2SiMe_3)_3(donor)_x$ at 30 °C in C_6D_6. Donor = $(THF)_2$, (DMPE)(THF), TMEDA, G_2 = diglyme, $(CH_3)_2(OCH_2CH_2)_2O$, G_3 = triglyme $(CH_3)_2(OCH_2CH_2)_3O$, DMPE = $Me_2PCH_2CH_2PMe_2$, TMEDA = $Me_2NCH_2CH_2NMe_2$

$RE(r)_3(donor)_x$	Label	$t_{1/2}$ [h]	Ref.
$Sm(CH_2SiMe_3)_3$(triglyme)	**Sm-triglyme**	0.7	This work
$Sm(CH_2SiMe_3)_3(THF)_3$	**Sm-THF**	2.8	19
$Sm(CH_2SiMe_3)_3$(diglyme)	**Sm-diglyme**	3.7	This work
$Y(CH_2SiMe_3)_3$(DMPE)(THF)	**Y-DMPE**	5.8	17
$Y(CH_2SiMe_3)_3$(triglyme)	**Y-triglyme**	7.8	This work
$Sc(CH_2SiMe_3)_3$(DMPE)	**Sc-DMPE**	9	This work
$Sm(CH_2SiMe_3)_3$(TMEDA)	**Sm-TMEDA**	11.7	This work
$Y(CH_2SiMe_3)_3$(diglyme)	**Y-diglyme**	24.4	This work
$Y(CH_2SiMe_3)_3$(TMEDA)	**Y-TMEDA**	36.5	17
$Sc(CH_2SiMe_3)_3(THF)_2$	**Sc-THF**	43.9	20
$Sc(CH_2SiMe_3)_3$(TMEDA)	**Sc-TMEDA**	73.4	This work
$Lu(CH_2SiMe_3)_3$(DMPE)(THF)	**Lu-DMPE**	74.1	This work
$Y(CH_2SiMe_3)_3(THF)_2$	**Y-THF**	119.6	This work
$Li[YCl(CH_2SiMe_3)_3(THF)_2]$	**LiClY-THF**	213	10
$Lu(CH_2SiMe_3)_3$(triglyme)	**Lu-triglyme**	190.7	This work
$Sc(CH_2SiMe_3)_3$(diglyme)	**Sc-diglyme**	258.1	This work
$Lu(CH_2SiMe_3)_3$(diglyme)	**Lu-diglyme**	278.2	This work
$Lu(CH_2SiMe_3)_3(THF)_2$	**Lu-THF**	482.6	15
$Lu(CH_2SiMe_3)_3$(TMEDA)	**Lu-TMEDA**	487.8	This work

$Lu(CH_2SiMe_3)_3(\kappa^2\text{-}G_1)$(THF) which the authors reported to be thermally robust but without providing data.[15] Most recently, *N*,*N* tetramethyl ethylene diamine (TMEDA) or bis-dimethylphosphino ethane (DMPE) have been reported to enhance the kinetic inertness of $[Y(CH_2SiMe_3)_3]$, with no further data.[17]

Herein, we report a comprehensive study of the relative thermal stabilities of nineteen rare earth complexes under conditions widely applied for protonolysis reactions, identifying the decomposition mechanisms, characterizing the important intermediates, and highlighting the importance of compound purity. We have prepared a library of seven known and twelve new solvated rare earth neosilyl complexes $M(r)_3(donor)_x$ for r = CH_2SiMe_3 (Fig. S5–S30, S55, and S56†) that cover a range of rare earth radii, between Sc ($r_{cov,\ 6\text{-coord}}$ = 0.745 Å) and Sm ($r_{cov,\ 6\text{-coord}}$ = 0.958 Å);[18] tris(CH_2SiMe_3) adducts with measurable stability at room temperature have not been made yet for any RE larger than Sm.[2,19] Previously reported complexes are: $M(r)_3(THF)_2$; M = Sm(III),[19] Y(III),[10] Lu(III),[15] Sc(III);[20] $Y(r)_3$(donor);[17] donor = DMPE/THF, TMEDA. The new complexes added here are: $M(r)_3(G_2)$; M = Sm(III), Y(III), Lu(III), Sc(III); $M(r)_3(G_3)$; M = Sm(III), Y(III), Lu(III); $M(r)_3$(TMEDA); M = Sm(III), Lu(III), Sc(III); $M(r)_3$(DMPE)(THF); M = Lu(III), Sc(III); G_2 = diglyme, $(CH_3)_2(OCH_2CH_2)_2O$, G_3 = triglyme $(CH_3)_2(OCH_2CH_2)_3O$ (Table 1). For simplicity we have abbreviated them here to a label that describes the metal and donor solvent, *i.e.* $M(r)_3$(donor) = **M-donor**. Single crystal X-ray data for all new compounds (except **Sm-G_2** and **Sm-G_3**) are discussed in the ESI (Tables S1–S10 and Fig. S31–S40).†

Results and discussion

Thermal stability and mechanistic studies

In a typical thermolysis experiment, 9.1 mM of a M complex is dissolved in C_6D_6 with hexamethylbenzene as an internal standard, in a J. Young NMR tube and the solution monitored by ^{1}H NMR spectroscopy for at least two half-lives during incubation at 30 °C.

Each compound's thermal stability is expressed as a half-life $t_{1/2}$ [h] of the complex in solution. Since all three mechanisms result in the formation of $SiMe_4$ (Scheme 1), the half-life (time for 50% of the compound to be converted into $SiMe_4$) is determined from linearized plots of the relative integration of the $SiMe_4$ resonance (Table 1) against hexamethylbenzene (Fig. S41–S45†). We first examined the half-life as a function of the metal center's ionic radius in M-THF and found a stability trend in the order $Sm^{3+} < Sc^{3+} < Y^{3+} < Lu^{3+}$ (Table 1). The low thermal stability of **Sm-THF** is in line with its large size, and metals with ionic radii larger than Sm do not afford isolable neosilyl complexes.[17,21]

Notably, the stability trend Sc < Y < Lu is in line with the metals' Lewis-acidity rather than size.[22]

We examined the thermal decomposition mechanism of diamagnetic **Lu-THF** in greater depth. The compound decomposes with a half-life of $t_{1/2}$ = 482.6 h. Kinetic studies using initial rates methods are first-order in [**Lu-THF**] suggesting an intramolecular decomposition process. We prepared the d_2-r, d_8-r, and d_9-THF labelled isotopomers of **Lu-THF** (Fig. S48†).

First, α-H elimination can be ruled out based on the decomposition studies on $Lu(d_2\text{-r})_3(THF)_2$ and $Lu(d_9\text{-r})_3(THF)_2$ since NMR spectra show resonances corresponding to d_2-and d_{10}-

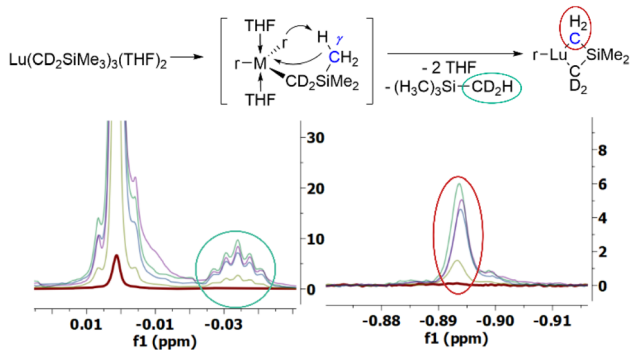

Fig. 1 Proposed γ-H elimination route converting $Lu(d_2\text{-}r)_3(THF)_2$ to the metallacycle that is visible in NMR spectra of the d_2-congener, with sections of the ^{1}H NMR spectra below measured at t = 0 h (red), 78 h (orange), 103 h (purple), 127 h (green), 165 h (violet) in C_6D_6, 30 °C. The resonance circled in green and red show the increase of $SiMe_3(CD_2H)$ and the $-CH_2$ group of a d_2-metallacyclic species, respectively.

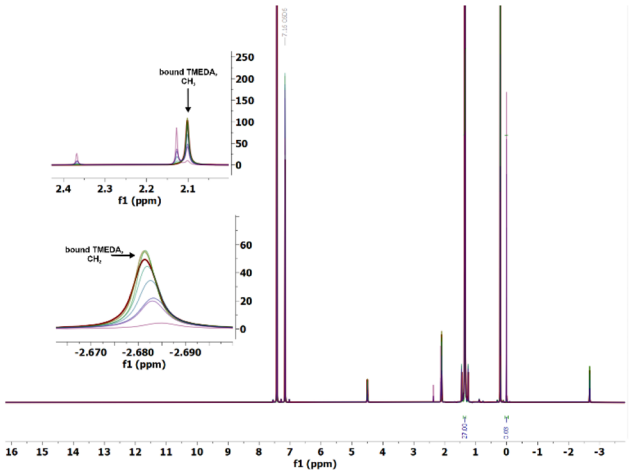

Fig. 2 ^{1}H NMR spectrum (600 MHz) of **Sm-TMEDA** in d_6-benzene (t = 28 h) showing $SiMe_4$ and TMEDA release.

labelled $SiMe_4$ as decomposition products, respectively (Fig. 1, and S48, inset†). This strongly suggests γ-H elimination as the primary decomposition mechanism, Scheme 1c. We measured a primary KIE = 2.09 for $Lu(d_9\text{-}r)_3(THF)_2$ (Fig. S53†) and no discernible KIEs for $Lu(r)_3(d_8\text{-}THF)_3$ or $Lu(d_2\text{-}r)_3(THF)_2$.

The thermolysis of **Lu-THF**, determined from the disappearance of the CH_2 neosilyl resonance, proceeds with a rate (9×10^{-4} h^{-1}) that is similar to that of $SiMe_4$ formation (11×10^{-4} h^{-1}), in agreement with decomposition *via* the liberation of 1 equiv. of $SiMe_4$ per **Lu-THF**. The slight discrepancy between the rates of **Lu-THF** consumption and $SiMe_4$ formation can be explained by an increasing resonance at $\delta = -0.894$ in ^{1}H NMR spectrum that overlaps with the CH_2 – neosilyl resonance at $\delta = -0.891$ (Fig. 1, and S49†). We assigned the growing resonance to the μ-CH_2 of the formed metallacycle $Me_2Si(\mu\text{-}CH_2)_2\text{-}LuCH_2SiMe_3$, (circled red in Fig. 1 and S49†), since the resonance is almost coincident with the $LuCH_2SiMe_3$ resonance, and can be observed in the ^{1}H NMR spectrum of $Lu(d_2\text{-}r)_3(THF)_2$.

Donor – dependence of RE-alkyl thermal stability

We initially synthesized **Lu-G$_2$**, which is *fac-pseudo* octahedral at Lu in solution and the solid-state (Fig. S9, S10, and S35†) to target an increased thermal stability of **Lu-THF** by sterically disfavoring γ-H elimination. However, a kinetic study reveals that decomposition occurs *via* γ-H elimination from the glyme rather than from the neosilyl, which is reasonable considering the greater acidity of the glyme CH_2 groups, decreasing the compound's half-life to $t_{1/2}$ = 278.2 h (Table 1, and Scheme 2). The same destabilizing effect is observed for **Y-G$_2$**. The size-fit correlation trend is supported by the observed increase in thermal stability for **Sc-G$_2$**, which showed a negligible activation of the glyme CH_2 groups (~1.48% glyme decomposition by release of CH_2=CHOMe[23] into solution, Fig. S46, and S47†) granting the compound with an approximately six-fold increased half-life ($t_{1/2}$ = 258.1 h) than **Sc-THF** ($t_{1/2}$ = 43.9 h). Somewhat surprisingly to us, the destabilization is even more pronounced for Sm, Y, and Lu adducts of the larger glyme **M-G$_3$** (Table 1). To target stable complexes of larger Ln that are desirable synthesis precursors, we made **M-donor** for M = Sm, Y, Lu, Sc and donor = TMEDA, DMPE, recognizing both have less acidic CH_2 groups than **G$_2$** and **G$_3$**. This increases the half-life by a factor of up to four for **Sm-TMEDA** ($t_{1/2}$ = 11.7 h). Notably, the kinetic study shows that **Sm-TMEDA** decomposes cleanly with release of one equiv. of $SiMe_4$ (Fig. 2). Therefore we expect this will be an excellent precursor for protonolysis reactions. In contrast to **M-TMEDA**, all the **M-DMPE** congeners showed shorter half-lives compared to their THF counterparts (Table 1).

^{1}H NMR studies on the d_9-labelled isotopomers of $Lu(r)_3(sol)$ (sol = diglyme, TMEDA, DMPE) (Fig. S50–S53†) indicate thermal decomposition *via* γ-CH activation as shown by the emergence of a 1 : 1 : 1 triplet resonance that can be assigned to $SiMe_3(CH_2D)$.

Impact of LiCl on the thermal stability and reactivity of the RE alkyls

While $M(r)_3(THF)_x$ (M = Sc, Lu; x = 2 and Sm; x = 3) were shown to decompose according to a first-order rate law in complex, our

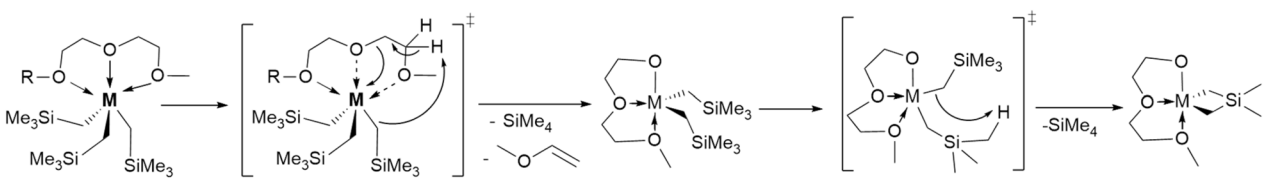

Scheme 2 Suggested route to the hypothesized ethoxyether-stabilised Lu silametallacycle from **Lu-diglyme**.

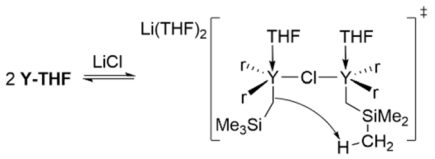

Scheme 3 Suggested route for the decomposition of LiCl-incorporated Y-THF that accounts for the observed kinetics.

initial experiments indicated a second-order rate-law for decomposition of the Y^{III} congener. This was supported by crossover studies on equimolar reaction mixtures of the d_2-r and d_9-r labelled complexes (Scheme S1, and Fig. S54†). All the reported routes to **Y-THF** originate from Li(r)[6,10] (Table S11†). We note that crystal structures of LiCl – free, neutral homoleptic $M(r)_3(THF)_x$ (M = Y, Lu, Yb, Er, Ho) have been reported.[10,14,24] While the previous reports did not discuss whether ^{7}Li NMR spectra were measured. However, we observed no resonance under normal conditions in ^{7}Li NMR spectroscopic studies of solutions.

The addition of 12-crown-4 ether (12-*c*-4) to a C_6D_6 solution of **Y-THF** results in a species we assign as Li(12-*c*-4)YCl(r)$_3$(THF)·(12-*c*-4)$_{1.75}$, which shows a ^{7}Li NMR resonance at $\delta = -2.09$ (Fig. S57†)[23] and an ^{1}H NMR spectrum that is different to the known Y(r)$_3$(12-*c*-4) (Fig. S58, and S59†).[25] In contrast, 12-*c*-4 addition to Lu(r)$_3$(THF)$_2$ solutions shows no change in the (silent) ^{7}Li NMR spectrum.

ICP – OES analyses combined with titration for chloride content (Mohr's method) indicate that **Y-THF** prepared from the reagent Li(r) is contaminated with 7% LiCl. This content explains why samples isolated in previous reports were able to 'pass' elemental analyses for carbon and hydrogen content (Table S11†). The use of elemental analysis to confirm bulk purity of a sample of a new complex has been the subject of recent scrutiny.[26,27]

We examined the effect of increasing the amount of incorporated LiCl from zero to 1 equiv. on the properties of **Lu-THF** in benzene solution. We observe a factor of 2.5 increase in the half-life ($t_{1/2}$) of the complex from $t_{1/2}$ = 482 h for **Lu-THF** to $t_{1/2}$ = 1122 h (Fig. S63†). It is notable that the chemical shifts of the THF CH_2 groups are significantly shifted to higher frequencies in both the ^{1}H – & ^{13}C NMR spectra compared to those of the alkyl groups. We suggest that in benzene solution at higher concentrations the THF is preferentially binding to Li and the Cl to the RE center, (Fig. S61, and S62†). Although the LiCl impurity improves the complexes' half-lives,[28,29] we expect it to hamper reactivity.

The inclusion of LiCl in s- and p-block alkyl complexes has been shown to significantly influence their stability, speciation, and reaction rates.[28] Knochel and co-workers have demonstrated that organomagnesium and organozinc compounds, in the presence of alkali metals, exhibit increased basicity, allowing them to deprotonate otherwise inert aromatic and heteroaromatic C–H bonds.[30] The combination of Grignard reagents with LiCl, known as turbo Grignard reagents, marks a significant advancement in main-group organometallic chemistry, leading to more accessible Grignard-like compounds that enable more powerful and controlled reactions. Recent *ab initio* molecular dynamics simulations suggest that LiCl aggregates form through μ_2-Cl bridging ligands, creating Li_4Cl_4 cubane-like structures in THF solutions.[29]

The observation of second-order kinetics described above for the decomposition of our Li(r)-prepared **Y-THF** suggests the facile formation of a chloride bridged intermediate shown in Scheme 3, as a potential deviation from the mechanism found for the pure alkyls.

Finally, a new route to pure **Y-THF** from Na(r)[31] is described in this work. As anticipated, ICP analyses and Mohr's method rule out LiCl or NaCl contamination of the complex, which decomposes following first order kinetics, with a $t_{1/2}$ = 119.6 h, compared with $t_{1/2}$ = 213 h for **Y-THF** prepared from Li(r) (Fig. S60, S64–S66,† and Table 1).

Conclusions

A new range of synthetically useful, more kinetically inert rare earth neosilyl solvates has been developed, based on the study of known and new solvates $M(CH_2SiMe_3)_3(sol)_n$, where M = Sc(III), Y(III), Lu(III), Sm(III), and sol = THF, TMEDA, DMPE, diglyme (G_2), and triglyme (G_3). The donor adduct with the longest half-life has been identified for each metal and is: **Sc-G$_2$**, 258 h; **Y-THF**, 120 h, **Lu-TMEDA**, 488 h; **Sm-TMEDA**, 12 h at room temperature. Samarium is the largest rare earth cation that we have been able to stabilise as a tris(r) adduct by adding simple donors.

Notably, simply increasing the denticity of donors to sterically hinder neosilyl γ-H elimination proves ineffective, as poorly fitting donors lead to new decomposition pathways. A precise size match with polydentate ligands can dramatically improve half-lives, as observed with **Sc-G$_2$**. However, when the fit is less optimal, alternative decomposition mechanisms, such as γ-H activation at a glyme CH_2 group, become more prominent. Thus, **Sc-donor** shows a significant increase in half-life when switching donor from THF (44 h) to diglyme (258 h), but **Lu-donor** shows a significant decrease in half-life when switching donor from THF (483 h) to diglyme (278 h). The stability trend of Sc < Y < Lu within the **M-THF** solvate series aligns more with Lewis acidity than size.

The incorporation of LiCl into the system results in an increase in half-life, particularly for **Lu-THF** by a factor of 2.5, although the effect on reactivity, particularly protonolysis, has not yet been evaluated.

Furthermore, while neutral complexes such as Lu(r)$_3$(sol) (sol = THF, TMEDA, DMPE, G_2) exhibit first-order kinetics involving γ-C–H activation, as confirmed by labelling experiments, ate complexes follow second-order kinetics, likely due to μ-Cl incorporation. Finally, a new route to pure **Y-THF** from Na(r) is described. While **Y-THF** exhibits a lower thermal stability compared to **LiClY-THF**, we expect it to open new perspectives for clean and fast protonolysis relevant to rare earth synthetic chemistry and catalysis.

Experimental

Materials and methods

All moisture and air sensitive materials were manipulated using standard high-vacuum Schlenk-line techniques and MBraun

gloveboxes and stored under an atmosphere of dried and deoxygenated argon. All glassware items, cannulae and Fisherbrand 1.2 μm retention glass microfiber filters were dried in a 160 °C oven overnight before use. $M(CH_2SiMe_3)_3(THF)_2$; M = Y(III),[10] Lu(III),[15] Sc(III)[20], $Sm(CH_2SiMe_3)_3(THF)_3$,[19] and $Y(CH_2SiMe_3)_3$(donor);[17] donor = (DMPE)(THF), TMEDA and $NaCH_2SiMe_3$ (ref. 31) were prepared according to published literature procedures and characterized with ^1H and ^7Li NMR spectroscopy.

n-Hexane, tetrahydrofuran (THF), diethyl ether (Et_2O) and toluene for use with moisture and air sensitive compounds were dried using an MBRAUN SPS 800 Manual solvent purification system and stored over activated 3 Å molecular sieves. Benzene-d_6 was purchased from Cambridge Isotope Laboratories and refluxed over potassium metal for 24 hours, freeze–pump–thaw degassed and purified by trap-to-trap distillation prior to use. THF-d_8 was purchased from Cambridge Isotope Laboratories and dried over sodium/benzophenone before being freeze–pump–thaw degassed and purified by trap-to-trap distillation prior to use. Diglyme ($(CH_3)_2(OCH_2CH_2)_2O$, **G_2**) was dried over sodium metal before freeze–pump–thaw degassed and purified by trap-to-trap distillation prior to use. Triglyme $(CH_3)_2(OCH_2CH_2)_3O$, **G_3**) was dried over sodium metal before being purified by dynamic vacuum distillation prior to use. Tetramethylethylenediamine (TMEDA) was dried over sodium before being freeze–pump–thaw degassed and purified by trap-to-trap distillation prior to use. 1,2-Bis(dimethylphosphino)ethane (DMPE) was purified by trap-to-trap distillation and stored over 3 Å molecular sieves.

All solvents were purchased from Sigma-Aldrich or Fisher Scientific and stored over 3 Å molecular sieves for at least 12 hours before being used.

Selected synthetic procedures (all other data in the ESI†)

Synthesis of LiCl-free $Y(CH_2SiMe_3)_3(C_4H_8O)_2$ (Y-THF). In an Ar-filled glovebox, anhydrous YCl_3 (26 mg, 0.133 mmol) was suspended in 260 mL THF and 2.6 mL 1 : 1 mixture of Et_2O and pentane. The resulting white suspension was cooled to −78 °C and $NaCH_2SiMe_3$ (ref. 31) (44 mg, 0.4 mmol, 3 eq.) was added portion wise as a solid. After stirring the resulting white suspension for 1 h at −78 °C, it was warmed to room temperature for 15 min. Filtration and removal of the solvent at −40 °C yielded the title compound as a white crystalline solid. Yield: 28 mg, 44% based on Y.

^1H NMR (600 MHz, C_6D_6) δ 3.88 (s, 8H), 1.34–1.32 (m, 8H), 0.30 (s, 27H), −0.68 (d, J = 2.7 Hz, 6H). ^{13}C NMR (151 MHz, C_6D_6) δ 70.60, 33.88, 33.65, 25.13, 4.63.

Anal. calcd for $YC_{20}H_{49}Si_3O_2$: C, 48.55; H, 9.98. Found: C, 48.43; H, 9.81.

Determination of chloride content. In an Ar-filled glovebox, **Y-THF** (6.7 mg) was weighed out in a 4 mL glass vial. The solid was then dissolved in water (4 mL) suitable for trace metal analyses, followed by the addition of a potassium chromate indicator (9.1 mg). A 25 mM solution of silver nitrate was titrated against the solution, resulting in the formation of silver chloride as white precipitates. The titration continued until the endpoint was reached, indicated by the formation of a dark orange solid (silver chromate) (Fig. S63†). The chloride content was determined to be ∼7.6%, which matched the Li content found by ICP analysis.

Synthesis of $Y(CH_2SiMe_3)_3(C_6H_{14}O_3)$ (Y-G_2). In an Ar-filled glovebox, anhydrous YCl_3 (100 mg, 0.512 mmol) was suspended in 3 mL THF at 60 °C overnight. Following evaporation of the solvent, the residue was re-suspended in pentane (4 mL). The white suspension was cooled down to −78 °C and a solution of $LiCH_2SiMe_3$ (146 mg, 1.55 mmol, 3 eq.) in pentane (2 mL) was added dropwise. The resulting reaction mixture was stirred for 1 h at room temperature, filtered and treated with diglyme ($(CH_3)_2(OCH_2CH_2)_2O$, **G_2**) (68.7 mg, 0.51 mmol), yielding $Y(CH_2SiMe_3)_3(C_6H_{14}O_3)$ (**Y-G_2**) as colorless crystalline solids. Diffraction quality crystals of $Y(CH_2SiMe_3)_3(C_6H_{14}O_3)$ (**Y-G_2**) were grown over three days from a saturated hexane solution at −40 °C. Yield: 51%, based on Y.

^1H NMR (600 MHz, C_6D_6) δ 3.07 (s, 6H), 2.97 (s, 4H), 2.68 (s, 4H), 0.44 (s, 27H), −0.42 (d, J = 2.9 Hz, 6H). ^{13}C NMR (151 MHz, C_6D_6) δ 69.18, 67.97, 60.68, 35.42 (d, J = 36.5 Hz), 4.78.

Anal. calcd for $YC_{18}H_{47}Si_3O_3$: C, 44.60, H, 9.77. Found: C, 42.37; H, 9.16.

Synthesis of $Sc(CH_2SiMe_3)_3(C_6H_{14}O_3)$ (Sc-G_2). In an Ar-filled glovebox, $Sc(r)_3(THF)_2$ (40.35 mg, 0.0895 mmol) was dissolved in 2.5 mL hexane. The yellowish solution was cooled down to −78 °C followed by addition of diglyme ($(CH_3)_2(OCH_2CH_2)_2O$, **G_2**) (100 μL, 0.716 mmol, 8 eq.) resulting in yellow precipitates which were extracted with hexane (3 × 2 mL). The combined hexane extracts were concentrated under reduced pressure and cooled down to −40 °C, yielding diffraction quality crystals of $Sc(CH_2SiMe_3)_3(C_6H_{14}O_3)$ (**Sc-G_2**) after six days. Yield: 54%, based on $Sc(r)_3(THF)_2$.

^1H NMR (600 MHz, C_6D_6) δ 3.23 (t, J = 5.2 Hz, 3H), 3.02 (s, 6H), 2.76 (t, J = 5.3 Hz, 5H), 0.41 (s, 36H), 0.09 (s, 6H). ^{13}C NMR (151 MHz, C_6D_6) δ 70.05, 69.71, 60.73, 4.33.

Anal. calcd for $ScC_{18}H_{47}Si_3O_3$: C, 49.05, H, 10.75. Found: C, 48.97; H, 10.66.

Synthesis of $Sm(CH_2SiMe_3)_3(C_6H_{14}O_3)$ (Sm-G_2). In an Ar-filled glovebox, anhydrous $SmCl_3$ (45.62 mg, 0.178 mmol) was suspended in 2.5 mL THF at room temperature for 20 min. Following the evaporation of the solvent, the residue was re-suspended in a 1 : 1 mixture of pentane and Et_2O (2.8 mL). The white suspension was cooled down to −78 °C and a solution of $LiCH_2SiMe_3$ (50.2 mg, 0.533 mmol, 3 eq.) in pentane (1.5 mL) was added dropwise. The resulting reaction mixture was stirred for 2 h at room temperature. The yellow filtrate was evacuated cold (−40 °C), the residues extracted with pentane (3 × 2 mL) and diglyme ($(CH_3OCH_2CH_2)_2O$, **G_2**) (22.7 mg, 0.16 mmol) added to the filtrate to yield $Sm(CH_2SiMe_3)_3(C_6H_{14}O_3)$ (**Sm-G_2**) as a yellow crystalline solid after storage overnight at −40 °C. Yield: 41%, based on Sm.

^1H NMR (600 MHz, C_6D_6) δ 5.46 (s, 6H), 5.29 (s, 6H), 0.44 (s, 27H), −0.14 (s, 4H), −1.53 (s, 4H). ^{13}C NMR (151 MHz, C_6D_6) δ 131.79, 31.97, 23.05, 14.34, 2.84.

Anal. calcd for $SmC_{18}H_{47}Si_3O_3$: C, 39.58, H, 8.67. Found: C, 39.29; H, 8.30.

Synthesis of $Lu(CH_2SiMe_3)_3(C_6H_{14}O_3)$ (Lu-G_2). In an Ar-filled glovebox, anhydrous $LuCl_3$ (49.5 mg, 0.176 mmol) was

suspended in 2.5 mL of tetrahydrofuran (THF) and heated to 50 °C for 40 min. After the solvent was evaporated, the residue was re-suspended in 2 mL of pentane. This white suspension was then cooled to −78 °C. Subsequently, a solution of $LiCH_2SiMe_3$ (50.2 mg, 0.533 mmol, 3 eq.) in 1.5 mL of pentane was added dropwise. The resulting reaction mixture was stirred for 2 hours at −78 °C. After being filtered while still cold, diglyme ($(CH_3)_2(OCH_2CH_2)_2O$, **G_2**) (23.6 mg, 0.176 mmol, 1 eq.) was added to the filtrate. This process yielded white crystalline solids with a yield of 60%, based on Lu. Finally, diffraction-quality crystals were grown from a concentrated solution of diethyl ether (Et_2O) and hexane at −40 °C.

^{1}H NMR (600 MHz, C_6D_6) δ 3.04 (s, 6H), 2.96 (t, J = 5.3 Hz, 4H), 2.61 (t, J = 5.3 Hz, 4H), 0.44 (s, 27H), −0.66 (s, 6H). ^{13}C NMR (151 MHz, C_6D_6) δ 69.41, 68.43, 60.70, 41.60, 4.91.

Anal. calcd for $LuC_{18}H_{47}Si_3O_3$: C, 37.88, H, 8.30. Found: C, 37.54; H, 8.13.

Synthesis of $Y(CH_2SiMe_3)_3((CH_3)_2(OCH_2CH_2)_3O)$ (Y-G_3). In an Ar-filled glovebox, anhydrous YCl_3 (586 mg, 3 mmol) was suspended in 10 mL of THF at 60 °C overnight. Following evaporation of the solvent, the residue was re-suspended in pentane (20 mL). The white suspension was cooled down to −78 °C and a solution of $LiCH_2SiMe_3$ (856 mg, 9.09 mmol, 3 eq.) in pentane (5 mL) was added dropwise. The reaction mixture was stirred at room temperature for 1 h. After stirring, it was cooled down to −78 °C, at which temperature it was filtered. The resulting mixture was treated with triglyme ($(CH_3)_2(OCH_2CH_2)_3O$, **G_3**) (534.7 mg, 3 mmol) at −78 °C. The result of this process was a white solid. This solid was then extracted using cold hexane (4 × 5 mL). From the combined saturated hexane fractions, diffraction quality crystals of $Y(CH_2SiMe_3)_3((CH_3)_2(OCH_2CH_2)_3O)$ were grown at −40 °C. The yield of this entire process was 56%, a calculation based on Y.

^{1}H NMR (400 MHz, C_6D_6) δ 3.47 (s, 6H), 3.09 (t, J = 4.8 Hz, 4H), 3.03–2.93 (m, 8H), 0.39 (s, 27H), −1.00 to −1.15 (m, 6H). ^{13}C NMR (151 MHz, C_6D_6) δ 72.32, 71.98, 69.51, 68.37, 5.27, 4.92.

Anal. calcd for $YC_{20}H_{51}Si_3O_4$: C, 45.43, H, 9.72. Found: C, 45.38; H, 9.76.

Synthesis of $Sm(CH_2SiMe_3)_3(CH_3)_2(OCH_2CH_2)_3O$ (Sm-G_3). In an Ar-filled glovebox, anhydrous $SmCl_3$ (140 mg, 0.545 mmol) was suspended in 1.1 mL THF at room temperature for 20 min. Following the evaporation of the solvent, the residue was re-suspended in a 1 : 1 mixture of pentane and Et_2O (8.4 mL). The white suspension was cooled down to −78 °C and a solution of $LiCH_2SiMe_3$ (146.5 mg, 1.556 mmol) in pentane (1.6 mL) was added dropwise. The resulting yellow reaction mixture was stirred for 2 h at room temperature. After stirring, it was cooled down to −78 °C at which temperature it was filtered. The yellow filtrate was evacuated cold (−40 °C), the residues were extracted with pentane (3 × 5 mL), and triglyme ($(C_8H_{18}O_4)$, **G_3**) (92.4 mg, 0.52 mmol) was added to the combined fractions yielding $Sm(CH_2SiMe_3)_3((CH_3)_2(OCH_2CH_2)_3O)$ (**Sm-G_3**). Yield: 48%, based on Sm.

^{1}H NMR (600 MHz, C_6D_6) δ 10.25 (s, 1H), 6.00 (s, 1H), 1.39 (s, 6H), −1.80 (s, 1H), −3.79 (s, 1H). ^{13}C NMR (151 MHz, C_6D_6) δ 152.17, 86.66, 72.19, 70.77, 69.74, 67.62, 58.73, 3.61.

Anal. calcd for $SmC_{20}H_{51}Si_3O_4$: C, 40.7, H, 8.71. Found: C, 40.32; H, 8.43.

Synthesis of $Lu(CH_2SiMe_3)_3((CH_3)_2(OCH_2CH_2)_3O)$ (Lu-G_3). In an Ar-filled glovebox, anhydrous $LuCl_3$ (154.8 mg, 0.550 mmol, 1 eq.) was suspended in 1.1 mL THF at 50 °C for 2 h. Following evaporation of the solvent, the residue was re-suspended in pentane (4.4 mL) and Et_2O (4.4 mL). The white suspension was cooled down to −78 °C and a solution of $LiCH_2SiMe_3$ (155.5 mg, 1.651 mmol, 3 eq.) in pentane (1.5 mL) was added dropwise. The cold well was lowered and the resulting reaction mixture was allowed to gradually warm with stirring over 1 h, then cooled down to −40 °C at which temperature it was filtered. Solvent was removed under vacuum. Following extraction with pentane at −40 °C (3 × 5.5 mL), triglyme ($(C_8H_{18}O_4)$, **G_3**) (98.1 mg, 0.550 mmol, 1 eq.) was added to the filtrate, yielding white crystalline solids. The resulting pentane supernatant was stored at −40 °C overnight, yielding diffraction quality crystals of $Lu(CH_2SiMe_3)_3((CH_3)_2(OCH_2CH_2)_3O)$ (**Lu-G_3**). Yield: 78.3 mg, 24% based on Lu.

^{1}H NMR (600 MHz, C_6D_6) δ 3.23 (t, J = 4.9 Hz, 4H), 3.13 (d, J = 8.5 Hz, 10H), 2.97 (t, J = 5.2 Hz, 4H), 0.42 (s, 27H), −0.82 (s, 6H). ^{13}C NMR (151 MHz, C_6D_6) δ 71.53, 69.69, 69.26, 60.51, 38.44, 34.45, 22.73, 14.27, 5.06.

Anal. calcd for $LuC_{20}H_{51}Si_3O_4$: C, 39.07, H, 8.36. Found: C, 38.69; H, 8.11.

Synthesis of $Sc(CH_2SiMe_3)_3(Me_2NCH_2CH_2NMe_2)$ (Sc-TMEDA). In an Ar-filled glovebox, $Sc(CH_2SiMe_3)_3(C_4H_8O)_2$ (45.6 mg, 0.101 mmol) was dissolved in 5 mL toluene and cooled to −40 °C in the glovebox freezer. To the cold clear yellow solution TMEDA (11.8 mg, 0.101 mmol, 1 eq.) in 3 mL toluene was added dropwise. The resulting clear yellow mixture was stirred for 1 h at room temperature. Toluene was removed under reduced pressure at room temperature. The remaining yellow oil was extracted with *n*-hexane (5 × 3 mL). The combined colorless extracts were filtered, concentrated and cooled to −40 °C, yielding colorless block shaped diffraction quality crystals of $Sc(CH_2SiMe_3)_3(Me_2NCH_2CH_2NMe_2)$ (**Sc-TMEDA**) overnight. Yield: 15 mg, 36% based on $Sc(CH_2SiMe_3)_3(THF)_2$.

^{1}H NMR (600 MHz, C_6D_6) δ 1.91 (s, 12H), 1.57 (s, 4H), 0.40 (s, 27H), 0.10 (s, 6H). ^{13}C NMR (151 MHz, C_6D_6) δ 56.85, 46.69, 16.93, 4.41.

Anal. calcd for $ScC_{18}H_{49}Si_3N_2$: C,51.13, H, 11.68; N, 6.63. Found: C, 50.97; H, 11.59; N, 6.57.

Synthesis of $Sm(CH_2SiMe_3)_3(Me_2NCH_2CH_2NMe_2)$ (Sm-TMEDA). In an Ar-filled glovebox, $Sm(CH_2SiMe_3)_3(C_4H_8O)_3$ (63.6 mg, 0.101 mmol) was dissolved in 5 mL toluene and cooled to −40 °C in the glovebox freezer. To the cold clear yellow solution TMEDA (11.8 mg, 0.101 mmol, 1 eq.) in 1 mL toluene was added dropwise. The resulting clear yellow mixture was stirred for 1 h at room temperature. Toluene was removed under reduced pressure at 0 °C. The remaining yellow oil was extracted with cold hexane. Removal of hexane at reduced temperature (−40 to 0 °C) yielded $Sm(CH_2SiMe_3)_3(Me_2NCH_2CH_2NMe_2)$ (**Sm-TMEDA**) as a yellow solid in 18% yield, 9.5 mg based on $Sm(CH_2SiMe_3)_3(THF)_3$.

^{1}H NMR (600 MHz, C_6D_6) δ 4.50 (s, 6H), 2.10 (s, 12H), 0.21 (s, 27H), −2.68 (s, 4H). ^{13}C NMR (151 MHz, C_6D_6) δ 58.45, 46.03.

Synthesis of $Lu(CH_2SiMe_3)_3(Me_2NCH_2CH_2NMe_2)$ (Lu-TMEDA). In an Ar-filled glovebox, $Lu(CH_2SiMe_3)_3(C_4H_8O)_2$ (58.6 mg, 0.101 mmol) was dissolved in 5 mL toluene and cooled to −40 °C in the glovebox freezer. To the cold clear colorless solution TMEDA (11.7 mg, 0.101 mmol, 1 eq.) in 3 mL toluene was added dropwise. The resulting clear colorless mixture was stirred for 1 h at room temperature. Toluene was removed under reduced pressure at room temperature. The remaining colorless solid was dissolved in hexane/Et_2O (2 mL, 1/1). The resulting solution was stored at −40 °C, yielding diffraction quality crystals of $Lu(CH_2SiMe_3)_3(Me_2NCH_2CH_2NMe_2)$ (**Lu-TMEDA**) after two days. Yield: 38 mg, 72% based on $Lu(CH_2SiMe_3)_3(THF)_2$.

^{1}H NMR (600 MHz, C_6D_6) δ 1.82 (s, 12H), 1.48 (s, 4H), 0.41 (s, 27H), −0.61 (s, 6H). ^{13}C NMR (151 MHz, C_6D_6) δ 56.60, 46.23, 45.51, 4.87.

Anal. calcd for $LuC_{18}H_{49}Si_3N_2$: C, 39.11, H, 8.93; N, 5.07. Found: C, 39.11; H, 8.97; N, 4.99.

Synthesis of $Sc(CH_2SiMe_3)_3(C_6H_{16}P_2)$ (Sc-DMPE). In an Ar-filled glovebox, $Sc(CH_2SiMe_3)_3(C_4H_8O)_2$ (45.5 mg, 0.101 mmol) was dissolved in 5 mL of toluene and cooled to −40 °C in the glovebox freezer. To the cold clear yellow solution bis(dimethylphosphino)ethane ($C_6H_{16}P_2$, DMPE) (15 mg, 0.101 mmol, 1 eq.) in 3 mL toluene was added dropwise. The resulting clear yellow mixture was stirred for 1 h at room temperature. Toluene was removed under reduced pressure at room temperature. The remaining yellow oil was extracted with *n*-hexane (5 × 3 mL). The combined colorless extracts were filtered, concentrated and cooled to −40 °C yielding colorless block shaped diffraction quality crystals of $Sc(CH_2SiMe_3)_3(C_6H_{16}P_2)$ (**Sc-DMPE**) after five days. Yield: 13 mg, 28% based on $Sc(CH_2SiMe_3)_3(THF)_2$.

^{1}H NMR (600 MHz, C_6D_6) δ 0.92 (s, 4H), 0.76 (t, J = 1.6 Hz, 12H), 0.40 (s, 27H), 0.26 (s, 6H). ^{13}C NMR (151 MHz, C_6D_6) δ 28.15, 14.04, 14.01, 13.97, 13.94. ^{31}P NMR (243 MHz, C_6D_6) δ −36.30.

Anal. calcd for $ScC_{18}H_{49}Si_3P_2$: C,47.33; H, 10.81. Found: C, 46.95; H, 10.56.

Synthesis of $Lu(CH_2SiMe_3)_3(C_6H_{16}P_2)(C_4H_8O)$ (Lu-DMPE). In an Ar-filled glovebox, $Lu(CH_2SiMe_3)_3(C_4H_8O)_2$ (58 mg, 0.101 mmol) was dissolved in 5 mL toluene and cooled to −40 °C in the glovebox freezer. To the resulting cold clear yellow solution 1,2-bis(dimethylphosphino)ethane ($C_6H_{16}P_2$, DMPE) (15 mg, 0.101 mmol, 1 eq.) in 3 mL toluene was added dropwise. The resulting clear colorless mixture was stirred for 1 h at room temperature. Toluene was removed under reduced pressure at room temperature. The remaining colorless solid was dissolved in a 1 : 1 mixture of hexane and Et_2O (2 mL). The resulting solution was stored at −40 °C, yielding diffraction quality crystals of $Lu(CH_2SiMe_3)_3$-$(C_6H_{16}P_2)(C_4H_8O)$ (**Lu-DMPE**) after three days. Yield: 41 mg, 60% based on $Lu(CH_2SiMe_3)_3(THF)_2$.

^{1}H NMR (600 MHz, C_6D_6) δ 3.91 (s, 4H), 1.36–1.28 (m, 4H), 1.12 (t, J = 7.0 Hz, 4H), 0.78 (s, 12H), 0.36 (s, 27H), −0.63 (s, 6H). ^{13}C NMR (151 MHz, C_6D_6) δ 25.13, 12.30, 4.77. ^{31}P NMR (243 MHz, C_6D_6) δ −38.88.

Anal. calcd for $LuC_{22}H_{57}Si_3P_2O$: C,40.1; H, 8.72. Found: C, 39.89; H, 8.62.

Data availability

The data supporting this article have been included as part of the ESI.† Crystallographic data are deposited at CCDC, codes 2351142–2351150, 2369795 and can be obtained from **https://www.ccdc.cam.ac.uk**.

Author contributions

ET, AB, MJ: experiments, analysis, writing & editing. PLA, JK, SP, PF: project conceptualization, funding acquisition, supervision, analysis, writing & editing.

Conflicts of interest

There are no conflicts to declare.

Acknowledgements

We thank Dow Chemical for support of this work. Some of the alkyl kinetic studies were also supported by the Catalysis Program of the U.S. Department of Energy (DOE), Office of Science, Office of Basic Energy Sciences, Chemical Sciences, Geosciences, and Biosciences Division at the Lawrence Berkeley National Laboratory under Contract DE-AC02-05CH11231. We thank Dr Cooper Citek and the Catalysis Laboratory in the DOE Catalysis Program for resource and instrumentation used in this work. We acknowledge the National Institutes of Health (NIH) for funding the UC Berkeley College of Chemistry NMR facility under grant no. S10OD024998 and the NIH Shared Instrumentation Grant S10-RR027172 for funding the UC Berkeley College of Chemistry Small Molecule X-ray Crystallography Facility (CheXray).

References

1 M. F. Lappert and R. Pearce, *J. Chem. Soc. Chem. Commun.*, 1973, 126, DOI: **10.1039/C39730000126**.
2 M. Zimmermann and R. Anwander, *Chem. Rev.*, 2010, **110**, 6194–6259.
3 M. Zimmermann, J. Takats, G. Kiel, K. W. Tornroos and R. Anwander, *Chem. Commun.*, 2008, 612–614, DOI: **10.1039/b713378b**.
4 S. Arndt, T. P. Spaniol and J. Okuda, *Angew. Chem., Int. Ed.*, 2003, **42**, 5075–5079.
5 C. Queffelec, F. Boeda, A. Pouilhès, A. Meddour, C. Kouklovsky, J. Hannedouche, J. Collin and E. Schulz, *ChemCatChem*, 2011, **3**, 122–126.
6 S. C. Kosloski-Oh, K. D. Knight and M. E. Fieser, *Inorg. Chem.*, 2023, **63**, 9464–9477.
7 J. Zhai, F. You, S. Xu, A. Zhu, X. Kang, Y.-M. So and X. Shi, *Inorg. Chem.*, 2022, **61**, 1287–1296.
8 P. L. Arnold, M. W. McMullon, J. Rieb and F. E. Kuhn, *Angew. Chem., Int. Ed.*, 2015, **54**, 82–100.
9 H. Liu, S. Saha and M. S. Eisen, *Coord. Chem. Rev.*, 2023, **493**, 215284.

10 S.-M. Chen, Y.-Q. Zhang, J. Xiong, B.-W. Wang and S. Gao, *Inorg. Chem.*, 2020, **59**, 5835–5844.
11 M. F. Lappert, in *Inorganic Compounds with Unusual Properties*, American Chemical Society, 1976, ch. 21, vol. 150, pp. 256–265.
12 D. J. H. Emslie, W. E. Piers, M. Parvez and R. McDonald, *Organometallics*, 2002, **21**, 4226–4240.
13 H. Schumann and J. Müller, *J. Organomet. Chem.*, 1979, **169**, C1–C4.
14 J. J. Carbó, D. García-López, M. Gómez-Pantoja, J. I. González-Pérez, A. Martín, M. Mena and C. Santamaría, *Organometallics*, 2017, **36**, 3076–3083.
15 K. A. Rufanov, D. M. M. Freckmann, H.-J. Kroth, S. Schutte and H. Schumann, *Z. Naturforsch. B Chem. Sci.*, 2005, **60**, 533–537.
16 A. R. Kennedy, J. Klett, R. E. Mulvey and D. S. Wright, *Science*, 2009, **326**, 706–708.
17 A. Mortis, C. Maichle-Mössmer and R. Anwander, *Dalton Trans.*, 2022, **51**, 1070–1085.
18 R. Shannon, *Acta Crystallogr., Sect. A: Cryst. Phys., Diffr., Theor. Gen. Crystallogr.*, 1976, **32**, 751–767.
19 H. Schumann, D. M. Freckmann and S. Dechert, *Z. Anorg. Allg. Chem.*, 2002, **628**, 2422–2426.
20 A. G. B. Getsoian, B. Hu, J. T. Miller and A. S. Hock, *Organometallics*, 2017, **36**, 3677–3685.
21 A. Mortis, F. Kracht, T. Berger, J. Lebon, C. Maichle-Mössmer and R. Anwander, *Dalton Trans.*, 2023, **52**, 44–51.
22 R. R. Golwankar, T. D. Curry II, C. J. Paranjothi and J. D. Blakemore, *Inorg. Chem.*, 2023, **62**, 9765–9780.
23 A. O. Tolpygin, A. S. Shavyrin, A. V. Cherkasov, G. K. Fukin and A. A. Trifonov, *Organometallics*, 2012, **31**, 5405–5413.
24 W. J. Evans, J. C. Brady and J. W. Ziller, *J. Am. Chem. Soc.*, 2001, **123**, 7711–7712.
25 S. Arndt, P. M. Zeimentz, T. P. Spaniol, J. Okuda, M. Honda and K. Tatsumi, *Dalton Trans.*, 2003, 3622–3627.
26 F. P. Gabbaï, P. J. Chirik, D. E. Fogg, K. Meyer, D. J. Mindiola, L. L. Schafer and S.-L. You, *Organometallics*, 2016, **35**, 3255–3256.
27 R. E. H. Kuveke, L. Barwise, Y. van Ingen, K. Vashisth, N. Roberts, S. S. Chitnis, J. L. Dutton, C. D. Martin and R. L. Melen, *ACS Cent. Sci.*, 2022, **8**, 855–863.
28 S. D. Robertson, M. Uzelac and R. E. Mulvey, *Chem. Rev.*, 2019, **119**, 8332–8405.
29 M. de Giovanetti, S. H. Hopen Eliasson, A. C. Castro, O. Eisenstein and M. Cascella, *J. Am. Chem. Soc.*, 2023, **145**, 16305–16309.
30 B. Haag, M. Mosrin, H. Ila, V. Malakhov and P. Knochel, *Angew. Chem., Int. Ed.*, 2011, **50**, 9794–9824.
31 D. E. Anderson, A. Tortajada and E. Hevia, *Angew. Chem., Int. Ed.*, 2023, **62**, e202218498.